Mat. Res. Soc. Symp. Proc. Vol. 674 © 2001 Materials Research Society

Ferromagnetic properties and Nanocrystallization behavior of Amorphous $(Fe_{0.99}Mo_{0.01})_{78}Si_9B_{13}$ Ribbons

Xiang-Cheng Sun[1,*], J. A. Toledo[1], S. Galindo[2] and W. S. Sun[3]

[1]Prog. Molecular Simulation, Instituto Mexicano del Petroleo, Lazaro Cardenas 152#, 07730, D.F. Mexico *E-mail: sun@imp.mx; Fax: +525-3336239
[2]ININ , Km.36.5, Carr. Mexico-Toluca, C.P.52045, Edo. de Mexico, Mexico.
[3]Institute of Metal Research, CAS, Shenyang, 110015, P. R. China

ABSTRACT

Ferromagnetic properties and nanocrystallization process of soft ferromagnetic $(Fe_{0.99}Mo_{0.01})_{78}Si_9B_{13}$ ribbons are studied by transmission electron microscope (TEM), X-ray diffraction (XRD), Mössbauer spectroscopy (MS), differential scanning calorimeters (DSC) and magnetization measurements. The Curie and crystallization temperature are determined to be T_C=665K and T_x = 750K, respectively. The T_x value is in well agreement with DSC measurement results. X-ray diffraction patterns had shown a good reconfirm of two metastable phases ($Fe_{23}B_6$, Fe_3B) were formed under in-situ nanocrystallization process. Of which these metastable phases embedded in the amorphous matrix have a significant effect on magnetic ordering. The ultimate nanocrystalline phases of α-Fe (Mo, Si) and Fe_2B at optimum annealing temperature had been observed respectively. It is notable that the magnetization of the amorphous phase decreases more rapidly with increasing temperature than those of nanocrystalline ferromagnetism, suggesting the presence of the distribution of exchange interaction in the amorphous phase or high metalloid contents.

INTRODUCTION

The very good promising bulk soft magnetic nanocrystalline (NC) materials, FeSiB based Finemet---are two phase alloys consisting of very fine BCC solid solution grains (typically with a diameter of about 10-15nm) embedded in a remaining amorphous matrix [1-5]. Yoshizawa [4] and co-workers revealed that the presence of small additions of Cu and Nb to some FeSiB-based alloys could allow the creation of two-phase materials by the devitrification, which showed superior soft magnetic properties. This effect was caused by the homogeneous precipitation of bcc α-Fe(*M*) nanocrystals embedded in the ferromagnetic amorphous matrix. Moreover, the addition of Cu, Nb had great influence on the formation of nanocrystalline materials by changing the crystallization behavior [3]. It can be expected that, study of crystallization of Fe-based metallic glasses containing transitional element additives will also benefit the development of new types of materials.

In the present work, by using transmission electron microscopy (TEM), differential scanning calorimeters (DSC), and X-ray diffraction (XRD), a study on nanocrystallization behavior had been carried out for $(Fe_{0.99}Mo_{0.01})_{78}Si_9B_{13}$ amorphous ribbons with a little amount of Mo element. Furthermore, intrinsic ferromagnetic properties were also studied using Mössbauer spectroscopy (MS) and vibrating sample magnetometer (VSM) techniques.

EXPERIMENT

Amorphous $(Fe_{0.99}Mo_{0.01})_{78}Si_9B_{13}$ (at%) alloy ribbons of 30mm width and about 25 μm thickness, were prepared by the melt-spinning techniques [6]. The transmission electron micrographs (TEM) were obtained with a JEOL-JEM100 EX electron microscopes, equipped with an *in situ* heating holder inside the electron microscope. The Mössbauer spectra were recorded using a conventional spectrometer of the electromechanical type with a $^{57}Co/Rh$ source. Differential scanning calorimetric measurements of the as-quenched ribbons were performed on a differential scanning calorimeter (DuPont 2000 Thermal Analysis DSC-2) using different heating rates under Ar gas atmosphere. X-ray diffraction (XRD) were carried out on a Simiens x-ray diffactometer (Cu, Kα radiation, λ=0.15418nm), Rietveld refinement was used to identify different phases. Magnetization measurements were carried out using a vibrating sample magnetometer (VSM) operating with applied magnetic fields up to 3600Oe from 16K to room temperature.

RESULTS and DISCUSSION

It should be noted that, two critical temperature points, crystallization temperature T_x and the Curie temperature T_c, usually determine the microstructure and their magnetic properties for Fe-based soft amorphous alloys. Consequently, it become very important to know this two critical temperature before our studying on $(Fe_{0.99}Mo_{0.01})_{78}Si_9B_{13}$ amorphous ribbons.

Fig. 1(a) shows the differential scanning calorimeters (DSC) thermal analysis for as-quenched ribbons samples at a heating rate of 10K/min. Two exothermic peaks are observed at around 768K and 803K, indicating this is typical primary crystallization process, in other words, two crystallization processes (nucleation and growth) took place, the around maximum of the first peak 750K reaches the crystallization temperature T_x for this $(Fe_{0.99}Mo_{0.01})_{78}Si_9B_{13}$ amorphous alloy.

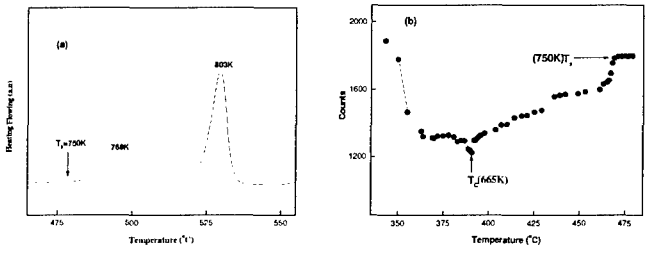

Figure 1 (a) DSC pattern at heating rate of 10K/min. Figure 1 (b). The Curie temperature determination using Mössbauer spectrometer

In order to determine the Curie temperature T_c, the velocity transducer of the Mössbauer spectrometer was set at zero velocity and counts were recorded for a fixed counting time, 15s, while the temperature was raised at a rate of 1K/min from 400K to 780K. The results are shown in Fig. 1 (b). The Curie temperature is determined to be 665K. As the temperature is further increased, the counts rate increase slowly due to the second-order Doppler effect [8],

and increase until 750K, then keep unchanged. In other words, the amorphous $(Fe_{0.99}Mo_{0.01})_{78}Si_9B_{13}$ alloy has reached the crystallization temperature T_x =750K, the amorphous state gradually transformed into the nanocrystalline phases. Both T_x and T_c values are in good agreement to previous measurements [6,7].

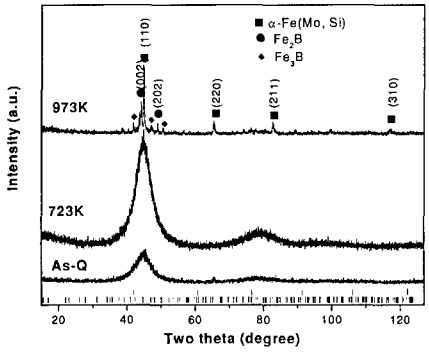

Figure 2 XRD patterns for as-quench $(Fe_{0.99}Mo_{0.01})_{78}Si_9B_{13}$ ribbon and two samples after 723K and 973K annealed treatments, respectively.

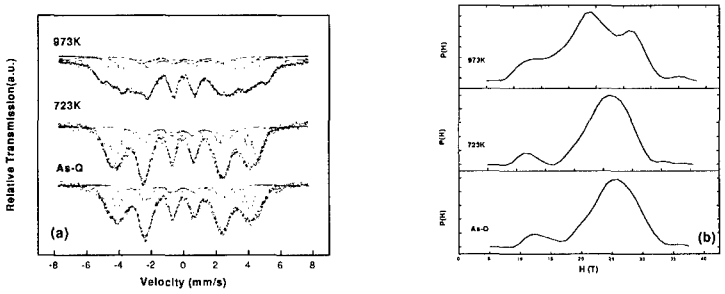

Figure 3 Mössbauer spectra (a) and hyperfine field distributions (b) for $(Fe_{0.99}Mo_{0.01})_{78}Si_9B_{13}$ ribbon and two samples after 723K and 973K annealed treatments, respectively.

Fig. 2 shows the XRD patterns for amorphous ribbon and two samples after 723K and 973K annealed treatments. It is clear to note that the as-quenched sample is in the amorphous state. On the heating the as quenched sample at 723K (T_C<T< T_x), very similar XRD pattern to amorphous state appears. However, very few metastable $Fe_{23}B_6$ (bcc), and Fe_3B (bct) borides phases are found using Rietveld XRD refinement analysis [6,7]. And from the following M□ssbauer spectra (Fig.3(b)), hyperfine field value is also seen to increase compared with amorphous sample. This phenomenon is mainly due to the internal strain

relaxation and short-range order that is induced by thermal treatment. On the another hand, after annealed the sample at temperature 973K than T_x ($T > T_x$), nanocrystalline phases (α-Fe(Mo, Si), Fe_2B, Fe_3B) are observed in the XRD pattern. Two main nanophases, α-Fe(Mo, Si) (bcc) and Fe_2B (bct), can be clearly identified.

The Mössbauer spectra and hyperfine field distribution of amorphous ribbon and the samples after 732K and 973K annealed treatment were shown in Fig.3 (a) and Fig.3 (b), respectively. And the fitted Mössbauer parameters of amorphous ribbon and the annealed samples were shown in table 1. The Mössbauer spectrum of amorphous $(Fe_{0.99}Mo_{0.01})_{78}Si_9B_{13}$ exhibits a magnetic pattern with a hyperfine magnetic field of 250 KOe and the broad lines are to be expected in view of the disordered atomic arrangements, in which the strength of the hyperfine interactions change from site to site due to the structurally inequivalent Fe environment. However, after annealed the amorphous sample at $T_C < T < T_x$, very few metastable $Fe_{23}B_6$ (bcc), and Fe_3B (bct) borides phases appeared, and the hyperfine field value (Fig.3 (b)) was also found to increase. It is expected that the observed increase in the hyperfine fields could be originated from the occurrence of the short-range order through redistribution of atoms and changes of its relative position in metastable Fe_3B(bct) and $Fe_{23}B_6$(bcc) phases during structural relaxation. Nevertheless, after annealed the amorphous sample at $T > T_x$, the Mössbauer spectrum consisted of two main magnetic patterns due to two nanophases, which confirmed by former XRD patterns of Fig.2. From Table 1, according to the literature reports [8, 9], the magnetic hyperfine field pattern of 308KOe and 246KOe belongs to bcc α-Fe(Mo, Si) solid solutions and bct Fe_2B boride, respectively.

In particular, the magnetization of the amorphous $(Fe_{0.99}Mo_{0.01})_{78}Si_9B_{13}$ have been measured at H_{app} = 3.6 KOe at various temperatures from 16K to RT. The results are shown in Fig. 4. It is clear that the magnetization M(T) / M(0) of the amorphous phase decreases more rapidly with reduced temperature T/T_C than those of α-Fe(Mo,Si) and Fe_2B nanocrystallines, which indicating the presence of the distribution of exchange interaction in the amorphous phase or high metalloid contents. And the saturation magnetization of the as-quenched amorphous materials extrapolated to 0K is found to be 2.01 μ_B/Fe atom. This value is smaller than the 2.22 μ_B of bcc Fe [10], suggesting that electron transfer from the metalloid atoms to the *d* band of the Fe atoms occur.

Table 1. The fitted Mössbauer parameters for $(Fe_{0.99}Mo_{0.01})_{78}Si_9B_{13}$ amorphous alloy and after different annealed treatment (H_{hf} is the magnetic hyper fine field, ΔE_Q is the quadrupole splitting, δ is the isomer shift and refers to α-Fe)

Annealed temperature (K)	**H_{hf} (KOe)**	**δ (mm/s)**	**ΔE_Q (mm/s)**
300	250.9±0.06	0.107±0.02	0.00±0.01
723	257.2±0.06	0.077±0.02	0.00±0.01
923	308.9±0.06	0.111±0.01	0.00±0.01
923	246.3±0.06	0.05±0.02	0.12±0.02

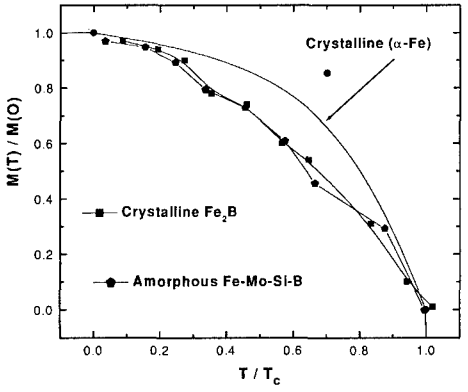

Figure 4. Reduced magnetization vs reduced temperature of the amorphous $(Fe_{0.99}Mo_{0.01})_{78}Si_9B_{13}$ ribbon and the α-Fe(Mo,Si) and Fe_2B nanocrystallines.

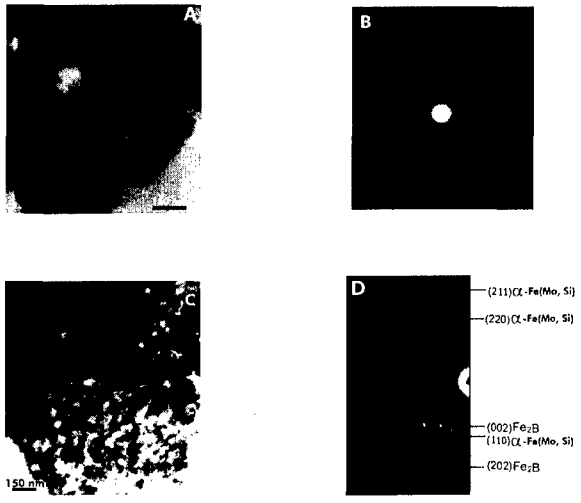

Figure 5 (a, b, c, d) Typical TEM morphologies and selected area electron diffraction for Fe-Mo-Si-B amorphous and nanocrystalline phases

Typical TEM images of the Fe-Mo-Si-B amorphous state and nanocrystalline alloy at annealing temperature, T_a = 973K ($T > T_x$), is shown in Fig.6 (a, b, c, d). From Fig.6 (c), small almost spherical nanometer grains precipitated homogeneously are observed. The selected area electron diffraction (Fig.6 (d)) patterns confirms that the randomly distributed nanocrystalline phases are crystalline α-Fe(Mo, Si) (bcc) and Fe_2B (bct) with a random orientation. Which is in good agreement with above XRD and Mössbauer analysis results.

CONCLUSIONS

Nanocrystalline Fe-Mo-Si-B alloys with different nanometer grain sizes have been successfully prepared by means of the *in situ* amorphous crystallization method. Two main nanophases are formed after full crystallization of the amorphous $(Fe_{0.99}Mo_{0.01})_{78}Si_9B_{13}$ alloy. The XRD pattern, M[]ssbauer spectra and in situ TEM observations suggest that the observed nanophases are the α-Fe(Mo, Si) (bcc) solid solution and the Fe_2B (bct).

The Curie temperature (T_c) and crystallization temperature (T_x) have been determined to be 665K and 750K using DSC thermal analysis and Mössbauer spectroscopy measurements. The reduced magnetization M(T)/ M(0) of the amorphous phase decreases more rapidly with reduced temperature T/T_C than α-Fe(Mo, Si) and Fe_2B nanocrystalline ferromagnetism, this kind of rapid decrease can be described in terms of either a distribution of exchange interaction in the amorphous phase or high metalloid contents.

ACKNOWLEDGMENTS

Financial support by the project No.01234 in IMP of Mexico is gratefully acknowledged. The authors would like to thank Dr. R. Hernadez for in-situ TEM observations; thank Dr. N. Nava for Mössbauer measurements; thank Mr. A. Morales for VSM measurements; thank Mr. Manuel for XRD analysis.

REFERENCES:

1. J. C. Rawers, R, A. McCune and A. Adams, *J. Mater. Sci. Lett.* **7**, 958 (1988)
2. A, Hernado, P. Marin, M. Vazquez, J. M. Barandiaran, and G. Herzer, *Phys. Rev.* **B58**, 366 (1998).
3. X. D. Liu, J. T. Wang and B. Z. Ding, *J. Mater. Sci. Lett.* **12**, 1108 (1993)
4. Y. Yoshizawa, S. Oguma and K. Yamauchi, *J. Appl. Phys.* **64**(10), 6044 (1988)
5. M. Bario, C. Antonione, P. Allia, P. Tiberto and F. Vinai, *Mater. Sci. Eng.* **A179**, 572 (1994).
6. X. D. Liu, K. Lu, and Z. Q. Hu, *Mater. Sci. Eng.* **A179/180,** 386 (1994)
7. H. Y. Tong, J. T. Wang, H. G. Jiang and K. Lu, *J. Non-Cryst. Solids* **150**, 444 (1992)
8. M. B. Sterns *Phys. Rev.* **129**, 1136 (1963)
9. C. S. Kim, S. B. Kim, J. S. Lee and T. H. Noh, *J. Appl. Phys.* **79**(8) 5459 (1996)
10. R. S. Tebble and D. J. Craik, *Magnetic Materials* (Wiley-Interscience, NewYork, 1969), P. 51